World Electric Vehicle Journal

Article

Fault Alarms and Power Performance in Hybrid Electric Vehicles Based on Hydraulic Technology

Zhuan You

School of Automobile and Transportation, Wuxi Institute of Technology, Wuxi 214121, China; youz@wxit.edu.cn

Abstract: In order to improve the fault alarm effect on the power performance of hydraulic hybrid electric vehicles (HEV), this paper proposes a fault alarm method for hybrid electric vehicle power performance based on hydraulic technology, builds a hybrid electric vehicle power system model, uses hydraulic technology to extract the characteristic signals of key components, uses support vector mechanisms to build a hybrid electric vehicle classifier, and obtains the fault alarm results for dynamic performance based on hydraulic technology. The results show that the proposed method can improve real-time diagnosis and alarm for engine faults in HEV, and the fault can be diagnosed after 5 s of injection, thus ensuring the dynamic stability of HEV.

Keywords: hydraulic technology; hybrid electric vehicle; dynamic performance; fault alarm; power system; support vector machine

check for updates

Citation: You, Z. Fault Alarms and Power Performance in Hybrid Electric Vehicles Based on Hydraulic Technology. *World Electr. Veh. J.* **2023**, *14*, 20. https://doi.org/10.3390/wevj14010020

Academic Editor: Vladimir Katic

Received: 1 November 2022
Revised: 9 January 2023
Accepted: 9 January 2023
Published: 10 January 2023

1. Introduction

With the advent of the information age, new technologies have been developed rapidly. In recent years, hydraulic hybrid technology has attracted increasing attention owing to its advantages of high power density, compact structure and low cost [1]. In hydraulic hybrid electric vehicles adopting this technology, the hydraulic hybrid transmission system can effectively recover the braking energy of the vehicle by utilizing the four-quadrant operating characteristics of the hydraulic pump/motor [2], so as to achieve the purpose of reducing energy consumption. The recovered energy can provide auxiliary power when the vehicle starts and accelerates, thus improving the dynamic performance of the vehicle, reducing the engine fuel consumption, reducing the emission of harmful substances, and improving the service life of the components of the vehicle braking system, which is especially suitable for frequent-start–stop urban vehicles [3]. Owing to the high power density of hydraulic accumulators (ACC) [4], hydraulic hybrid technology has greater advantages over hybrid electric technology for heavy-duty hybrid vehicles, especially in terms of vehicle starting, climbing and acceleration [5]. However, since the power system structure of hydraulic hybrid electric vehicles is more complex than that of traditional vehicles, there are more types and forms of power performance failures [6]. Among them, the most common types of power performance failures in hydraulic hybrid electric vehicles include engine failure, hydraulic accumulator failure and hydraulic pump/motor failure [7]. Therefore, it is necessary to develop a scientific method for dynamic performance fault identification and alarm in hydraulic hybrid electric vehicles so as to realize real-time identification and alarm of various dynamic performance faults under different working conditions [8].

In recent years, some scholars have studied the fault alarm method in electric vehicle dynamic performance and achieved some progress. For example, Chen et al. proposed the diesel engine fault diagnosis method [9], which uses an optimized stent autoencoder to extract the depth features of complex original signals and input them into the constructed diagnosis network to realize the diesel engine fault diagnosis. This method has high accuracy and high efficiency in the fault diagnosis of automobile diesel engines. However, it does not perform well in fault diagnosis for hydraulic hybrid power systems. He et al. proposed a fault diagnosis method for converters of series hybrid electric vehicles [10]. This method decomposes the classified power device's open-circuit fault signals into different frequency bands by fast Fourier transform. After analysis and comparison, the signal of a specific frequency band is selected as the fault diagnosis feature vector, based on which fault type identification can be realized by combining a genetic algorithm and a BP neural network. Although this method can reduce the diagnosis error effectively, it can only diagnose a single fault type, and the test range is not large enough. Zhang et al. [11] studied exponential wavelet thresholds and PSO-DP-LSSVM for engine bearing fault diagnosis. The wavelet threshold function was used to decompose and reconstruct the original signal, extract the energy characteristics of each component after noise reduction, and construct an LSSVM model to output the fault diagnosis results for engine bearings through training. This method improves the diagnosis accuracy for engine bearing fault signals, but the diagnosis accuracy for multi-joint faults needs to be further improved.

Aiming at the inaccurate judgment of fault types and inefficient early warnings with the above methods, this paper proposes a hybrid electric vehicle power performance fault alarm system based on hydraulic technology and establishes a dynamic performance multi-fault alarm model, in order to realize the dynamic performance fault alarm for electric vehicles.

2. Power Performance Fault Alarm for Hydraulic Hybrid Electric Vehicles

2.1. Power System Model for Hydraulic Hybrid Electric Vehicles

This paper constructs a power system model for hydraulic hybrid electric vehicles based on hydromechanical stepless transmission technology, which can not only realize the stepless change of transmission ratio, but also realize the effective recovery and reuse of braking energy. The vehicle power system model adopts planetary differential mechanism shunting and fixed gear pair convergence to realize speed decoupling and torque decoupling, so that the engine works in the high-efficiency area. The overall model structure of the power system of the hydraulic hybrid electric vehicle is shown in Figure 1.

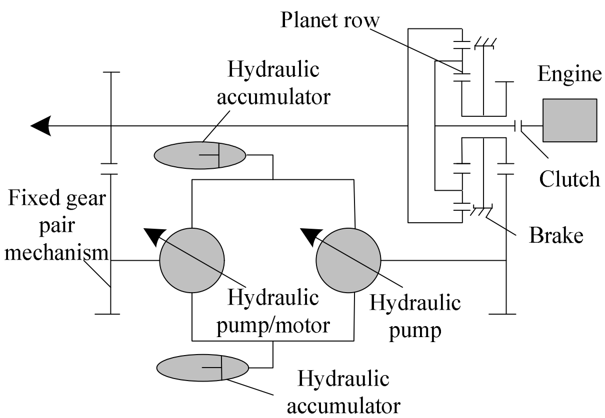

Figure 1. Overall model structure of the power system of the hydraulic hybrid electric vehicle.

As shown in Figure 1, the power system of the hydraulic hybrid electric vehicle is mainly composed of the engine, clutch, brake, planetary exhaust, hydraulic pump/motor, hydraulic accumulator and other parts. The planetary exhaust structure is mainly composed of three parts, including the solar wheel, planetary frame and gear ring. The planetary frame is connected to the engine as the input end, the sun wheel is connected to the hydraulic transmission part, and the gear ring is connected to the output part [12]. Through effective control of the engine, different working modes for the hydraulic hybrid electric vehicle can be realized.

2.1.1. Driving Model of the Power System of the Hydraulic Hybrid Electric Vehicle

In order to simplify the calculation, only the basic resistance overcome by the power system of the hydraulic hybrid electric vehicle is modeled. According to Newton's second law, the driving running resistance balance equation for the power system of the hydraulic hybrid electric vehicle is:

$$F_o = F_a + F_b + F_c + F_d \tag{1}$$

where F_o is the running resistance of the power system of the hydraulic hybrid electric vehicle; F_a is the wheel rolling resistance of the hydraulic hybrid electric vehicle; F_b is the driving air resistance of the hydraulic hybrid electric vehicle; F_c is the slope resistance of the hydraulic hybrid electric vehicle; and F_d is the starting overtaking acceleration resistance of the hydraulic hybrid electric vehicle. The total power requested by the power system of the hydraulic hybrid electric vehicle is:

$$P_{re} = v\delta_o F_o \tag{2}$$

where P_{re} is the total power requested by the power system of the hydraulic hybrid electric vehicle; δ_o is the transmission mechanical efficiency; and v is the speed of the hydraulic hybrid electric vehicle under cycle conditions. According to the driver behavior characteristics and vehicle dynamics characteristics, and by referring to the literature related to intelligent driving systems, a speed model of the vehicle under complex urban road conditions is established [13]. The speed profile model is shown in Figure 2.

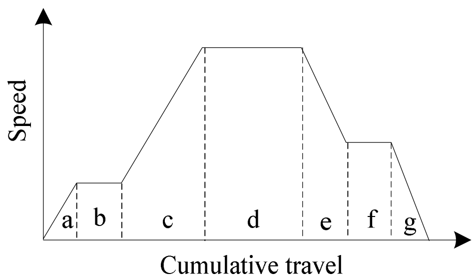

Figure 2. Velocity profile model.

In Figure 2, phase a is the acceleration phase, phase b is the speed-climbing phase, phase c is the acceleration-speed-setting phase, phase d is the specific-speed-holding phase, phase e is the deceleration phase, phase f is the deceleration-speed-holding phase, and phase g is the average-speed-descending phase.

2.1.2. Engine Model of Power System of Hydraulic Hybrid Electric Vehicle

The mathematical model of the engine parameters in the power system of the hydraulic hybrid electric vehicle is:

$$\begin{cases} v_1 = v\sigma_o\sigma_a/r \\ f_1 = p_1/v_1 \end{cases} \tag{3}$$

where f_1, p_1 and v_1 are the engine's power output shaft torque, the engine's power demand and the engine's crankshaft angular speed, respectively; σ_o and σ_a are the transmission ratio of the gearbox and the "main reduction and differential" gear ratio, respectively; and r is the wheel radius of the hydraulic hybrid vehicle. The model variable terms are shown in Table 1.

Table 1. Terms of model variables.

Variable Terminology	Definition	Unit
f_1	Output torque of power take-off	N·m
p_1	Force required for normal engine operation	N
v_1	The crankshaft is the most important part of the engine. It bears the force from the connecting rod and converts it into torque, which is outputted through the crankshaft to drive other accessories in the engine to work. The angular speed of the crankshaft refers to the speed at which the crankshaft moves around the center of the circle.	rad/s
σ_o	Ratio of the angular velocity of two rotating components, also called speed ratio.	-
σ_a	The circumference is the actual rolling distance of the wheel and is used to calculate the equivalent radius of the wheel when it rolls.	mm

The feedback control mathematical equation for the engine in the power system of the hydraulic hybrid electric vehicle is:

$$G_1 v_1 = f_1 - \phi_1 q_{acc} S_1 \times ({v_1}^{re} - v_1) \tag{4}$$

where G_1 is the moment of inertia of the engine power output shaft. The moment of inertia is a physical quantity, m^4, which is used to describe the ability of an object to resist twisting and torsion. The concentrated mass and moment of inertia of each part are modeled through automatically added mass and moment-of-inertia nodes; ϕ_1 is the control coefficient; q_{acc} is the instantaneous pressure of the accumulator; q_{acc} is the peak displacement of the engine-driven pump; ${v_1}^{re}$ is the engine's requested angular speed. Through the response of the control coefficient ϕ_1, the instantaneous output angular velocity of the engine in the power system of the hydraulic hybrid electric vehicle is adapted to the requested angular velocity, thus meeting the demand of load power.

2.1.3. Hydraulic Accumulator Model of the Power System of the Hydraulic Hybrid Electric Vehicle

As an energy storage unit in the power system of hydraulic hybrid electric vehicles, the hydraulic accumulator needs to quickly store or release energy to meet the braking or driving requirements of hydraulic hybrid electric vehicles. The hydraulic accumulator can store the recovered braking energy and convert the pressure energy into mechanical energy when the hydraulic hybrid electric vehicle accelerates or starts [14]. According to the working principles of the hydraulic accumulator, there is:

$$\begin{cases} q_{acc} V_1 = M_1 K T_1 \\ V_1 = \int_{V_{\min}}^{V_{\max}} Z_{acc} dt \\ q_{acc} = {}^{q_{\max} V_1}/{}_{V - V_1} \end{cases} \tag{5}$$

where V_1, M_1 and T_1 are the volume, mass and temperature of inert gases (such as nitrogen, etc.) in the hydraulic accumulator under instantaneous pressure q_{acc}, respectively; K is the inert gas constant. The permeability of inert gas in the tire is low, which can maintain the stability of tire pressure, reduce the probability of tire blowout, prolong the life of the tire, reduce the vibration of the tire on the uneven road surface, and allow the vehicle to run smoothly. Therefore, the modeling process is of great importance; $V_{\max}$ and $V_{\min}$ are the maximum and minimum oil volumes in the hydraulic accumulator, respectively; t is the time; Z_{acc} is the actual flow of the hydraulic accumulator; V is the total volume of the selected hydraulic accumulator; $q_{\max}$ is the maximum working pressure of the hydraulic accumulator. When the system pressure is lower than the internal pressure of the accumulator, the oil in the hydraulic accumulator flows to the external system under the action of high-pressure gas to release energy. The remaining amount Q_{SOC} of hydraulic energy in the hydraulic accumulator is shown as follows:

$$Q_{SOC} = {}^{(q_{acc} - q_{\min})}/_{(q_{\max} - q_{\min})} \tag{6}$$

where $q_{\min}$ is the minimum working pressure of the hydraulic accumulator (i.e., the minimum residual pressure of the hydraulic accumulator). If the hydraulic accumulator exceeds the maximum working pressure in actual operation, the hydraulic accumulator will stop working (i.e., stop being charged by the engine), so as to ensure the safety of the power system of the hydraulic hybrid electric vehicle. The thermodynamic model used in the above research process is the Boltzmann statistical distribution model.

2.1.4. Hydraulic Pump/Motor Model of the Power System of the Hydraulic Hybrid Electric Vehicle

For the power system of the hydraulic hybrid electric vehicle, the hydraulic pump/motor is a regenerative braking component as well as one of the driving components [15], so the hydraulic pump/motor must meet the following requirements:

(1) Under low-speed and low-load conditions, the hydraulic pump/motor can start the whole vehicle, respectively, to meet specified speed requirements within a certain time.

(2) The hydraulic pump/motor needs to meet the requirements for regenerative braking. For hydraulic hybrid vehicles, the hydraulic pump/motor is mainly responsible for recovering the braking energy during vehicle deceleration [16]. When the braking strength H = 0 $\leq$ 0.1, the hydraulic pump/motor is responsible for independent braking. When the braking strength H = 10.1 $\leq$ 0.7, the combined braking mode of the hydraulic regenerative braking system and mechanical braking system should be adopted. When the braking strength H = 2 > 0.7, the hydraulic pump/motor does not work, and the braking torque is solely provided by the mechanical braking system. Therefore, the hydraulic pump/motor should be selected on the premise that all braking torque is provided when h = 0.1, that is:

$$L_{p/m} = q_{\min} S_2^{\max} = {}^{0.1Nr_1}/_{\lambda_1 \lambda_{p/m}} \tag{7}$$

where $L_{p/m}$ is the torque of the hydraulic pump/motor; $S_2^{\max}$ is the maximum displacement of the hydraulic pump/motor; r_1 and N are the wheel rolling radius and total gravity of the hydraulic hybrid electric vehicle, respectively; λ_1 is the main reduction ratio of the drive axle; and $\lambda_{p/m}$ is the transmission ratio of the torque coupler. When the system efficiency and power change, the rolling radius will not change significantly, and can be basically ignored, so the impact of the rolling model and system power on the rolling radius is not considered.

(3) Under normal driving conditions, the hydraulic accumulator can be charged by adjusting the working point of the engine. When the charging pressure reaches the preset value, the whole hydraulic hybrid vehicle adopts hydrostatic driving mode, and the minimum power of the hydraulic pump/motor at the lowest pressure of the hydraulic accumulator should meet the power demands of the whole hydraulic hybrid vehicle at the average endurance speed, that is:

$$\left(P_{p/m}\right)_{\min} = \overline{v} F_\mu \left({}^{1}/_{3600\delta_{p/m}}\right) \tag{8}$$

where $P_{p/m}$ is the power of the hydraulic pump/motor; $\left(P_{p/m}\right)_{\min}$ is the minimum power of the hydraulic pump/motor; $\overline{v}$ is the average driving speed of the hydraulic hybrid electric vehicle; F_μ is the resistance overcome by the driving of hydraulic hybrid electric vehicle; and $\delta_{p/m}$ is the working efficiency of the hydraulic pump/motor. Excessive pressure and excessive flow in the hydraulic system are the fundamental causes of energy consumption. Therefore, it is necessary to reduce the pressure surplus, make the system pressure as close as possible to the load pressure, and reduce the flow surplus, so that the hydraulic system can save energy.

At the same time, the maximum power of the hydraulic pump/motor should meet the requirements of the hydraulic hybrid vehicle to drive at the maximum speed and climb at a certain speed, that is:

$$\begin{cases} (P_z)_{\max} = \max(P_{z1}, P_{z2}) \\ P_{z1} = v_{\max} F_\mu \left(1/3600\delta_z\right) \\ P_{z2} = v_2 \left(F_\mu + F_c\right) \left(1/3600\delta_z\right) \end{cases} \tag{9}$$

where $v_{\max}$ is the preset maximum driving speed of the hydraulic hybrid electric vehicle and v_2 is the climbing speed of the hydraulic hybrid vehicle.

2.2. The Power Performance Fault Alarm of the Hydraulic Hybrid Electric Vehicle Based on a Support Vector Machine

Based on the power system model and key component model for the hydraulic hybrid electric vehicle established in the previous section, a power performance fault alarm model for the hydraulic hybrid electric vehicle based on a support vector machine (SVM) has been constructed. Faults in key components in the power system of the hydraulic hybrid electric vehicle can be diagnosed in real time, and the alarm information can be sent in time to realize real-time diagnosis and alarm for single faults and multiple faults in the power performance of the hydraulic hybrid electric vehicle. The fault alarm model can realize the identification and alarm of different types of power performance faults in real time. Compared with the fault alarm system for only a single component, the established fault alarm model comprehensively considers the operation state of the power system of the hydraulic hybrid electric vehicle, and realizes diagnosis and alarm for all key components of the power system more accurately.

2.2.1. Feature Signal Extraction for the Key Components of Hydraulic Hybrid Electric Vehicle's Power System

Through the constructed power system model of the hydraulic hybrid electric vehicle, the characteristic signals of key components are extracted. After processing these characteristic signal data, data samples for key components of the power system are formed. Taking the data samples as the input samples, the power performance fault alarm model for the hydraulic hybrid electric vehicle based on support vector machine is constructed to realize the real-time diagnosis and alarm of power performance faults. Since all characteristic signals are derived from the simulation results for the power system model and key component model of the hydraulic hybrid electric vehicle, all extracted characteristic signals must be included in the model. Considering the compatibility of the alarm model and the whole vehicle controller of the hydraulic hybrid electric vehicle, the extracted characteristic signal can be regarded as the input signal for the controller of the hydraulic hybrid electric vehicle, that is, the characteristic signal that can be collected by the sensor in the actual hydraulic hybrid electric vehicle. The characteristic signals for key components of the hydraulic hybrid electric vehicle's power system to be extracted are shown in Table 2.

Table 2. Extraction of characteristic signals for key components of the power system of the hydraulic hybrid electric vehicle.

Key Component Name	Name and Unit of Characteristic Signal
The engine	Power/kW Rotate speed/r/min Torque/N/m
Hydraulic accumulator	Residual hydraulic energy Voltage/V Current/A
Hydraulic pump/motor	Torque/N/m Power/kW Rotate speed/r/min

The characteristic signal data for the key components of the hydraulic hybrid vehicle power system are extracted by a magnetoelectric sensor, and the processing of such characteristic signal data is realized by programming. The processing flow of characteristic signal data is shown in Figure 3.

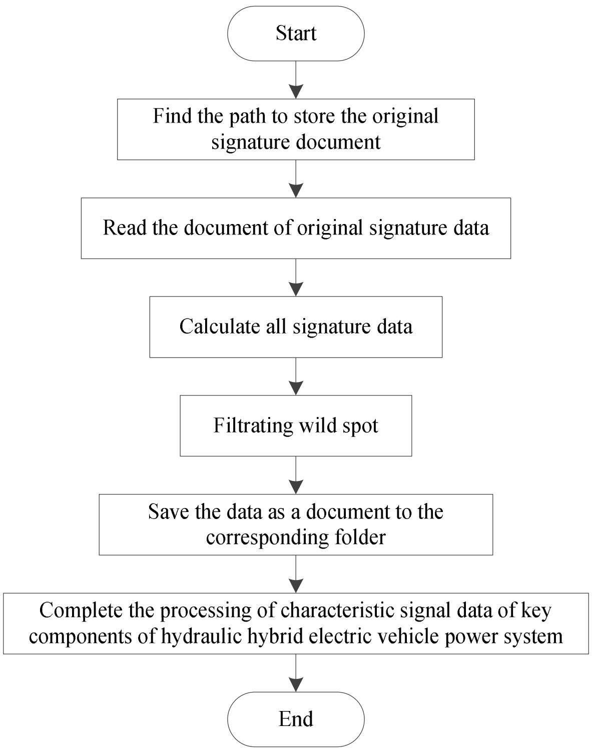

Figure 3. Processing flow for characteristic signal data.

Firstly, read the document of original characteristic signal data, find the path to store the file, take out one line at a time, and read successively until all characteristic data of the complete document are read. Then calculate all characteristic signal data, further analyze and process all characteristic data obtained, and filter out wild points, so as to ensure the accuracy of fault diagnosis and alarm in subsequent applications. Finally, all the dynamic characteristic data obtained are saved to corresponding folders to process the extracted characteristic signal data for key components of the hydraulic hybrid electric vehicle's power system.

2.2.2. Power Performance Fault Alarm Model of Hydraulic Hybrid Electric Vehicle

Taking the characteristic data for the key components processed above as the input samples and combining them with the support vector mechanism, the dynamic performance fault alarm model for the hydraulic hybrid electric vehicle is established. A support vector machine is essentially a binary classification algorithm as well as a kind of generalized linear classifier that classifies data in a binary way according to supervised learning. Its decision boundary is the maximum edge hyperplane for learning samples [17]. This classification algorithm is slightly inadequate for complex power systems that may have a variety of power performance fault modes [18], so it is necessary to build a multi-classifier support vector machine. This paper adopts the one-to-one (OVO) indirect method to realize the construction of multiple classifiers using a support vector machine. This method realizes the construction of multiple classifiers by combining two classifiers [19]. Aiming at three common power performance faults in the power system of hydraulic hybrid vehicles, such as engine operation faults, hydraulic accumulator internal resistance faults and hydraulic pump/motor faults, three different internal resistance faults in hydraulic accumulators are constructed. The classifiers are fault classifiers 1–2, engine operation fault–hydraulic pump/motor fault classifiers 1–3, and hydraulic accumulator internal resistance fault–hydraulic pump/motor fault classifiers 2–3, respectively. Among them, labels 1, 2 and 3 represent engine running faults, accumulator internal resistance faults and hydraulic pump/motor faults, respectively [20]. After two classifiers are constructed, the OVO indirect method is used to construct a multi-classifier for the support vector machine, and the input samples are inputted into the multi-classifier to construct the dynamic performance fault alarm model, so as to realize the fault detection of the input samples. The structure of the dynamic performance fault alarm model of the hydraulic hybrid vehicle is shown in Figure 4.

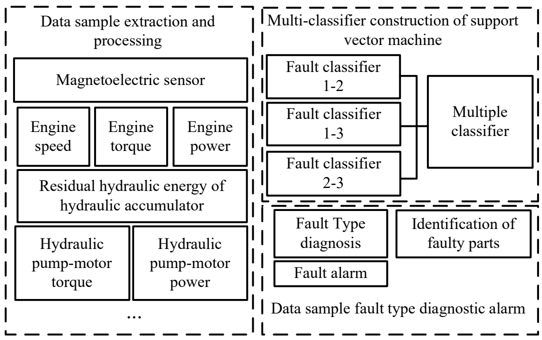

Figure 4. Structure diagram of the power performance fault alarm model of the hydraulic hybrid electric vehicle.

The dynamic performance fault alarm model of the hydraulic hybrid electric vehicle mainly has three functions, including the extraction and processing of characteristic data samples of the key components, the construction of the support vector machine multi-classifier and fault category diagnosis and alarm. The data samples are obtained from the established power system model and key component model of the hydraulic hybrid electric vehicle. The multi-classifier of the support vector machine is constructed by the OVO indirect method [21,22]. The fault diagnosis and alarm system outputs the fault category of data samples through the constructed multi-classifier of the support vector machine and sends out alarm information after confirming the fault components.

2.2.3. Design of the Power Performance Fault Alarm Process of the Hydraulic Hybrid Electric Vehicle

The fault alarm process for the power performance fault alarm of the hydraulic hybrid electric vehicle is shown in Figure 5.

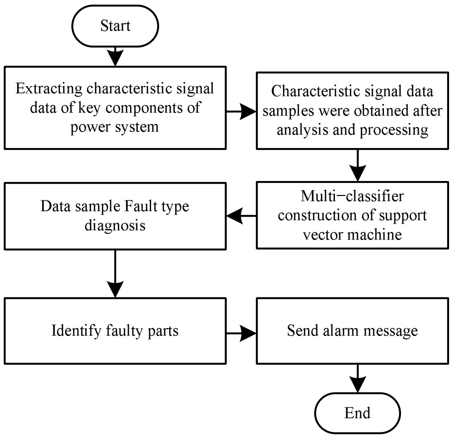

Figure 5. Power performance fault alarm process of the hydraulic hybrid electric vehicle.

The fault state is confirmed according to the count value, then the fault component is determined [23]. When the fault state of the fault type output by the multi-classifier of the support vector machine is non-0 (default), the counter increases by 1; when the fault state is 0 (non-default), the counter decreases by 1; when the counter value is between the given counter upper limit (TUL) and the given counter lower limit (tll), the actual counter value is outputted; when the counter value exceeds TUL, the TUL value is outputted; when the counter value is equal to TLL and the current fault state is 0, the TLL value is outputted; when the counter value is equal to TLL and the current fault state is 1, 0 is outputted; when the counter value reaches the upper limit of counting, the fault type state is confirmed, the fault state is outputted and the corresponding components are confirmed. TUL and TLL are 127 and 128, respectively, according to international standards for the vehicle's safety integrity level.

3. Experimental Results

In this experiment, magnetoelectric sensors were used to extract the characteristic signal data of key components of the hydraulic hybrid electric vehicle power system, including the engine, hydraulic accumulator, and hydraulic pump/motor. The long-line transmission isolator of PWM square wave signal conversion was adopted as the signal acquisition device, and the extracted characteristic signal was regarded as the input signal of the hydraulic hybrid electric vehicle controller.

Then locate the storage path of the file and read the file one line at a time until all the feature data of the complete file are read one line at a time. Save all the dynamic feature data to the corresponding folders and carry out data processing.

Finally, the fault diagnosis and alarm system outputs the fault data samples through the multi-classifier of the support vector machine and sends the alarm information for the corresponding fault parts.

In this paper, the main experimental equipment included the (a) transmission isolator, (b) Msensor, (c) magnetoelectric sensor, (d) engine, and (e) hydraulic pump/motor (see Figure 6).

Three common power performance faults, including engine operation faults, hydraulic accumulator internal resistance faults and hydraulic pump/motor faults are inputted into the experimental vehicle model. The method constructed in this paper is used to carry out real-time diagnosis and alarm for various power performance faults. The experimental vehicle model is shown in Figure 7.

The key parameters of the established experimental vehicle model are shown in Table 3.

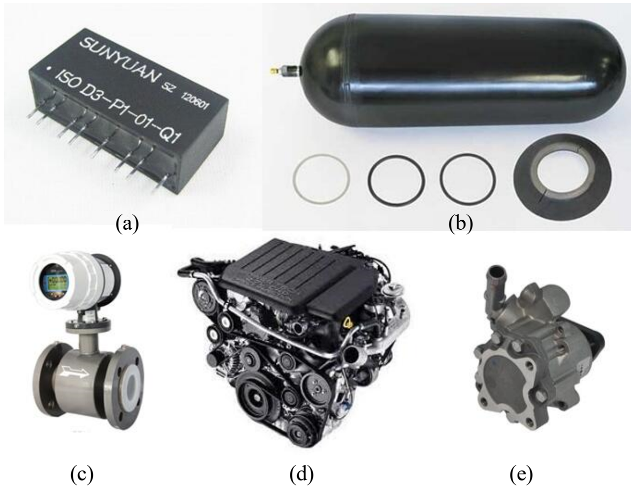

Figure 6. Main experimental equipment. (**a**) transmission isolator, (**b**) Msensor, (**c**) magnetoelectric sensor, (**d**) engine, and (**e**) hydraulic pump/motor.

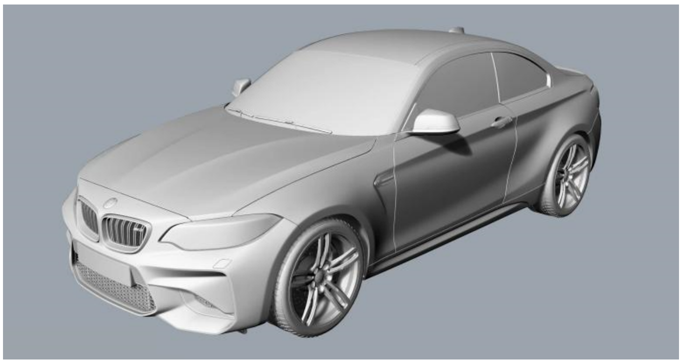

Figure 7. Experimental vehicle model.

Table 3. Key parameters of the experimental vehicle model.

The Parameter Name	Parameters of the Unit	Parameter Values
Vehicle rotation mass conversion coefficient	—	1.03
Vehicle-load quality	kg	1398
The wheel radius	cm	30
Coefficient of air resistance	—	0.34
Moment of inertia of hydraulic pump/motor	cm^4	0.52
Maximum speed of hydraulic pump/motor	r/min	4510
Minimum speed of hydraulic pump/motor	r/min	490
Windward area	cm^2	202
Coefficient of rolling resistance	—	0.013
Vehicle front wheelbase	cm	106
Rear wheelbase of vehicle	cm	140
The main transmission ratio	—	3.93
Maximum speed	km/h	158
Height of the center of mass	cm	59
Hydraulic pump/motor displacement	mL/r	57
Hydraulic pump/motor peak pressure	Mpa	46
Hydraulic accumulator charging pressure	Mpa	2.1
Initial volume of hydraulic accumulator	L	42
Engine rating	kW/(r/min)	55/5300

3.1. Alarm for Single-Type Power Performance Faults

3.1.1. Alarm for Internal Resistance Faults for the Hydraulic Accumulator

When the experimental vehicle model had run for 30 s, the internal resistance fault for the hydraulic accumulator was injected into the experimental vehicle model. The real-time alarm for internal resistance faults in the hydraulic accumulator was implemented using the proposed method, and the alarm effect for the internal resistance faults of the hydraulic accumulator was tested based on the actual alarm results. The variation in the running speed of the experimental vehicle model as well as the residual hydraulic energy Q_{SOC} of the hydraulic accumulator over time under fault injection and fault-free injection are shown in Figure 8.

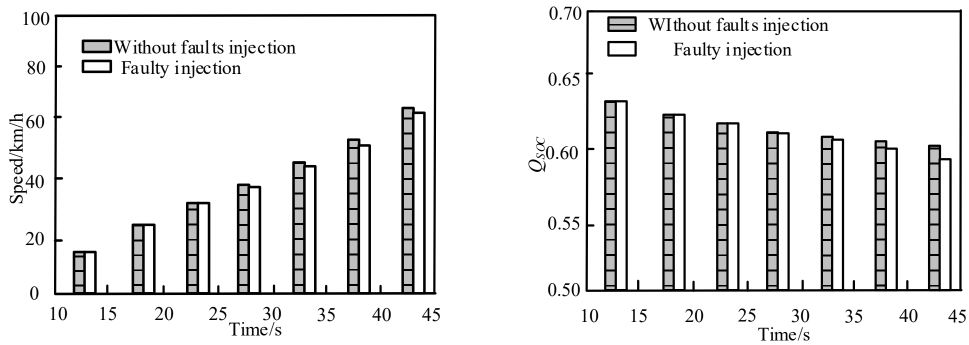

(**a**) (**b**)

Figure 8. Variation in driving speed and the remaining hydraulic energy of the hydraulic accumulator in the experimental vehicle model with and without faults. (**a**) Speed changes; (**b**) change in the remaining hydraulic energy of the hydraulic accumulator.

The real-time diagnosis and alarm results for the internal resistance fault of the hydraulic accumulator in the experimental vehicle model are shown in Figure 9.

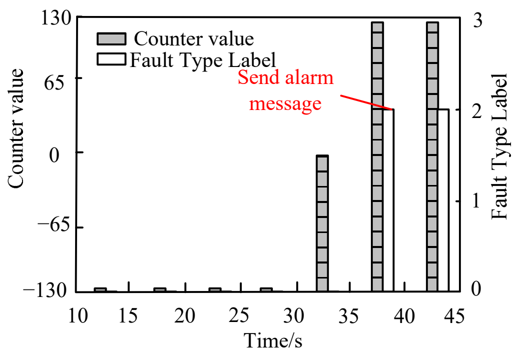

Figure 9. Real-time alarm results for the hydraulic accumulator's internal resistance failure by the proposed method.

It can be seen in Figures 8 and 9 that, compared with the injection of the hydraulic accumulator without an internal resistance fault, after an internal resistance fault injection in the hydraulic accumulator for 30 s, the increased amplitude of the driving speed of the experimental vehicle model became smaller and the decreased amplitude of the residual hydraulic energy of the hydraulic accumulator became larger due to the increase in internal resistance. This is because the hydraulic accumulator's internal resistance fault changed little within a few seconds after the initial injection, the proposed method diagnosed the fault 5 s after the injection of the hydraulic accumulator's internal resistance fault, and the counter value began to increase. After 5 s of fault confirmation, fault type label 2 was outputted and the alarm information was sent out, so as to realize the diagnosis and alarm of the hydraulic accumulator's internal resistance fault in real time.

It can be seen from the above data that the proposed system can realize an alarm for single-type power supply performance, and its fault response time is less than 5 s, indicating good application performance.

3.1.2. Alarming of Engine Operation Fault

According to the test vehicle data in Table 3, when the test vehicle ran for 45 s, the engine running fault code was inputted into the vehicle running program, so that the engine failed. Figure 10 shows the time-dependent changes in engine power and rotational speed of the test vehicle model under faulty injection and no-fault-injection conditions.

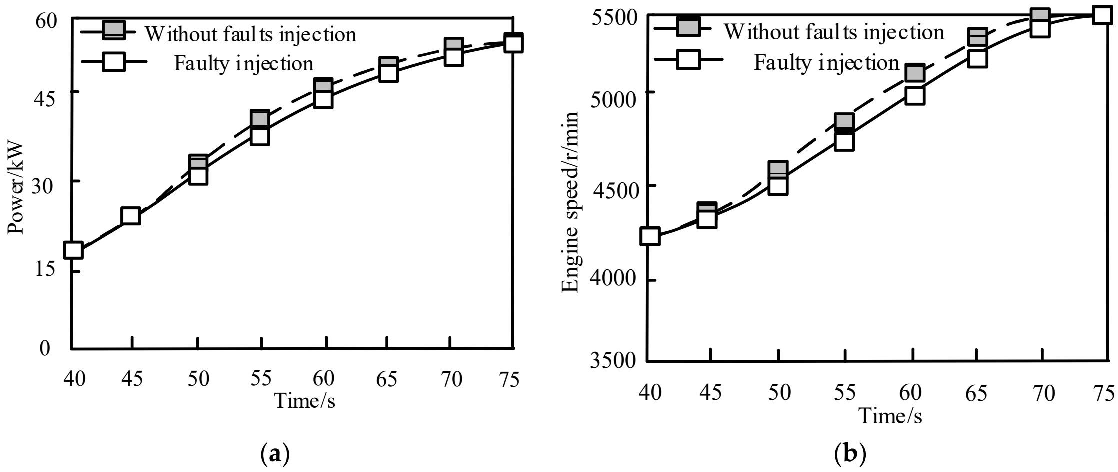

Figure 10. Changes in engine power and speed over time in experimental vehicle models with and without fault injection. (**a**) Engine power changes; (**b**) Engine speed changes.

The real-time diagnosis and alarm results for engine running faults in the experimental vehicle model are shown in Figure 11.

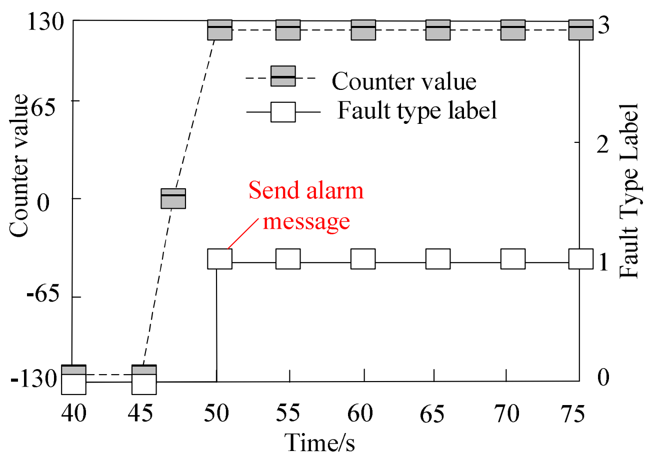

Figure 11. Real-time alarm results for engine operation faults by the proposed method.

It can be seen in Figures 10 and 11 that the engine operation fault sample data were injected when the experimental vehicle model ran for 45 s. It was found that the engine power and speed of the vehicle model were lower than those under normal operation, the increase in engine power and speed was smaller, and the time to reach the rated power and speed was longer; 2.5 s after fault injection, the proposed method diagnosed the occurrence of the fault, and the counter value started to increase. Five seconds after fault injection, the counter value reached the highest value, and the confirmation of fault type was completed. Fault type label 1 was outputted, and alarm information was sent, which is confirmed in the red font part of the figure. The proposed method is proved to be capable of outputting correct early warning information, indicating excellent fault diagnosis and early warning effects.

3.1.3. Detection of the Fault Alarm Effect for the Hydraulic Pump/Motor

After the experimental vehicle model ran for 90 s, the hydraulic pump/motor fault was injected into the experimental vehicle model. The real-time alarm for the hydraulic pump/motor fault was implemented using the proposed method, and the actual alarm effect of the method was tested based on the actual alarm results. Under fault injection and fault-free injection conditions, the time-dependent changes in driving speed and hydraulic pump/motor torque of the experimental vehicle model are shown in Table 4.

Table 4. Variation in the driving speed and hydraulic pump/motor torque of experimental vehicle models with and without faults.

Time/s	Without Fault Injection		With Fault Injection	
	Experimental Car Model Driving Speed/km/h	Hydraulic Pump/Motor Torque/N/m	Experimental Car Model Driving Speed/km/h	Hydraulic Pump/Motor Torque/N/m
80	21.33	510.05	21.33	510.05
85	32.05	301.25	32.05	301.25
90	39.85	245.32	39.52	245.29
95	45.68	225.16	43.16	225.12
100	50.55	218.56	46.47	216.13
105	58.73	206.35	52.35	201.45
110	60.14	196.58	53.08	195.23
115	63.17	185.06	55.57	184.98
120	65.06	177.95	58.96	177.91
125	68.73	170.65	60.51	170.62
130	70.05	166.56	63.47	166.53

The real-time diagnosis and alarm results for hydraulic pump/motor faults in the experimental vehicle model are shown in Figure 11.

It can be seen in Table 4 and Figure 12 that, after hydraulic pump/motor fault injection for 90 s, the driving speed and the increases amplitude of the experimental vehicle model gradually decreased due to the reduction in the mechanical efficiency and the driving capacity of the hydraulic pump/motor. At the same time, it can be seen that the torque of the hydraulic pump/motor after 90 s with fault injection decreased compared with that without fault injection, affecting the acceleration performance of the whole experimental vehicle model. After injection of the hydraulic pump/motor fault for 3 s, the proposed method diagnosed the fault and the counter value began to increase. After 6 s of fault injection, the counter value reached the highest value, the fault type confirmation was completed, the fault type label 3 was outputted and alarm information was sent out, so as to realize real-time diagnosis and alarm for hydraulic pump/motor faults in the experimental vehicle model.

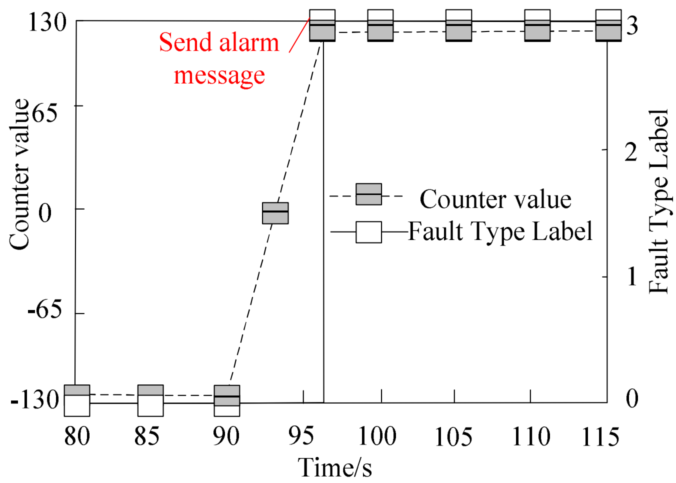

Figure 12. Real-time alarm results for hydraulic pump/motor faults by the proposed method.

3.2. The Alarm Effect for Multi-Type Power Performance Faults

The alarm effect for multi-type dynamic performance faults was detected under the conditions of faulty injection from 150 s to 160 s, hydraulic accumulator internal resistance fault from 165 s to 190 s, and hydraulic pump/motor fault from 195 s to 210 s. Real-time diagnosis and alarm for various types of dynamic performance faults were carried out using the proposed method. According to the actual alarm results, the alarm effect for multi-type dynamic performance faults using the proposed method was verified. Real-time diagnosis and alarm results for multi-type dynamic performance faults in the experimental vehicle model are shown in Figure 13.

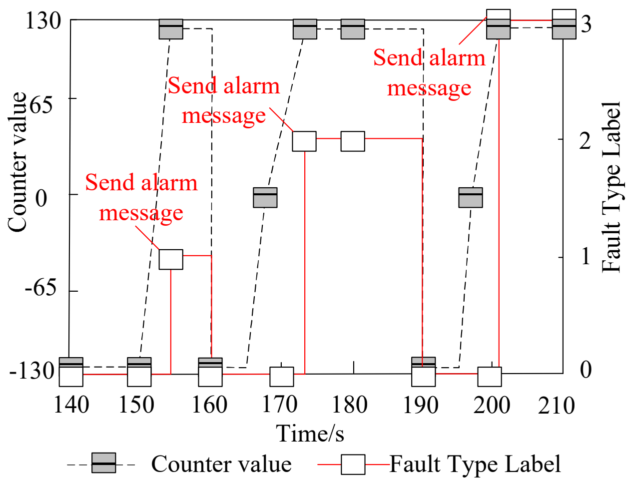

Figure 13. Real—time alarm results for multi-type faults by the proposed method.

As can be seen in Figure 13, the counter value for engine operation fault increased gradually from about 150 s, and reached the highest value after 5 s. It can be confirmed that the fault type was an engine operation fault; tag 1 was outputted and alarm information was sent out and the counter value decreased to the lowest value between 160 s and 165 s. When the internal resistance fault for the hydraulic accumulator was injected at 165 s, the counter value rose again and reached its highest value at 173 s. It can be confirmed that the fault type was an internal resistance fault of the hydraulic accumulator; tag 2 was outputted and alarm information was sent out. The counter value was kept at the lowest value between 190 s and 195 s, and then increased gradually after the hydraulic pump/motor fault injection until the highest value of the counter was reached at 201 s. It can be confirmed that the fault type was a hydraulic pump/motor fault; tag 3 was outputted and alarm information was sent out.

The fault classification accuracies for the support vector machine multi-classifiers constructed by the OVO indirect method, the method in [10] and the method in [11] are comparatively analyzed, and their ROC curves are shown in Figure 14.

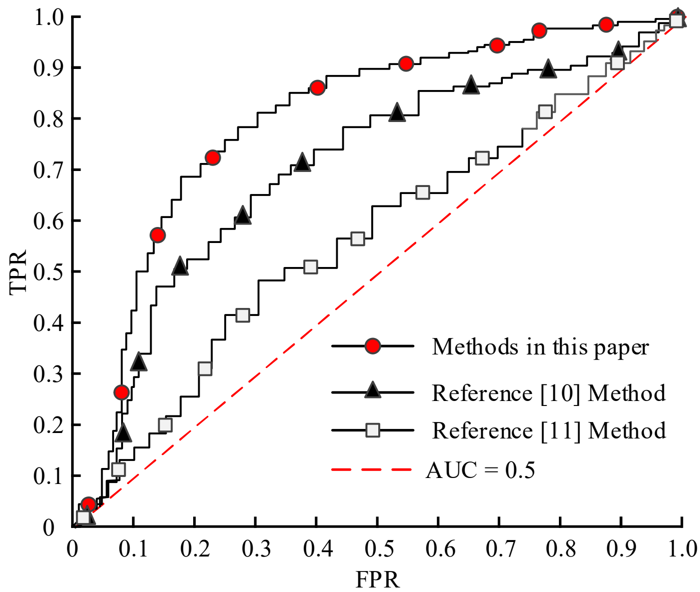

Figure 14. ROC curve of fault classification [10,11].

According to the AUC values of the three fault classification algorithms in Figure 14, the proposed support vector classifier has the highest classification accuracy.

The fault classification effects of the proposed method, the method in [10] and the method in [11] were comparatively analyzed, and the results are shown in Figure 15.

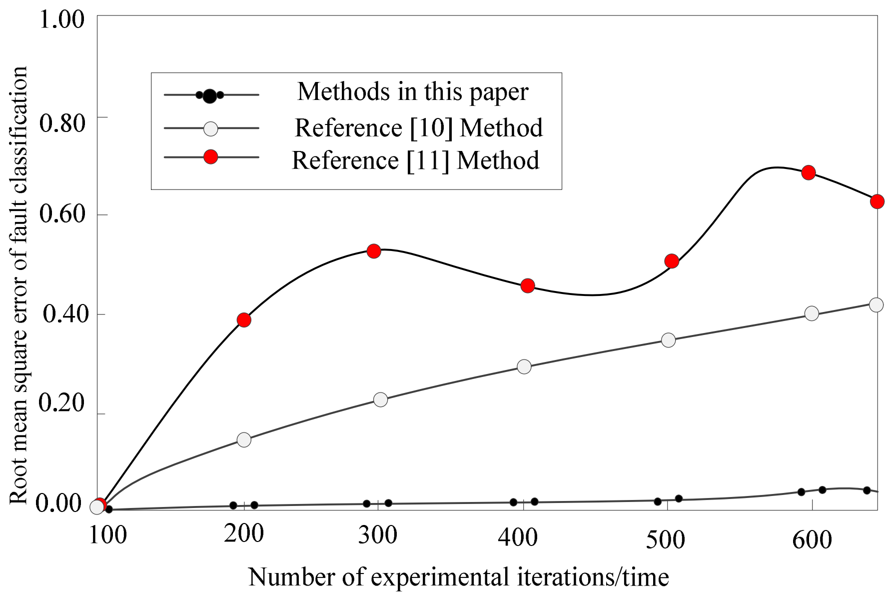

Figure 15. Root-mean-square error of fault classifications [10,11].

According to Figure 15, when the number of experiments is 200, the root-mean-square errors of fault classification for the method in [10], the method in [11], and the proposed method are 0.13, 0.39, and 0.01, respectively. When the number of experiments is 500, the root-mean-square errors of the fault classification for the method in [10], the method in [11], and the proposed method are 0.35, 0.53, and 0.03, respectively. The above results show that the proposed method is more effective in classifying electric vehicles' dynamic performance faults.

In summary, the proposed method has fast response ability and strong fault confirmation ability for the above three types of power faults. The diagnosis and alarm rate for the proposed method is higher for engine running faults and hydraulic pump/motor faults, but slightly lower for hydraulic accumulator internal resistance faults. However, further study is needed to investigate the reason why the proposed method takes a longer time to alarm for t internal resistance faults in the hydraulic accumulator.

4. Conclusions

This paper proposes a dynamic performance fault alarm method for hydraulic hybrid electric vehicles. The proposed method has the function of not only analyzing dynamic performance faults but also diagnosing key components in the hydraulic hybrid electric vehicle power system in real time. The fault response time for the proposed method is short, usually less than 5 s. However, the proposed fault alarm method is only applicable for diagnosis and alarm for three key faults, including engine running faults, hydraulic accumulator internal resistance faults and hydraulic pump/motor faults. In the future, we will continue to study the diagnosis and alarm effect for other types of power failures in the power systems of hydraulic hybrid electric vehicles.

Funding: The research was supported by the "Qinglan Project" Funding Project of Jiangsu Colleges and Universities (No. 3, [2019]) and the Research Project of Professor or Doctor in Wuxi Institute of Technology (BT2020-10).

Institutional Review Board Statement: This article does not contain any studies with human participants performed by any of the authors.

Informed Consent Statement: Not applicable.

Data Availability Statement: All data generated or analysed during this study are included in this published article.

Conflicts of Interest: The author declares no conflict of interest.

References

1. Hou, S.; Yin, H.; Ma, Y.; Luo, R. Energy Management Strategy of Hybrid Electric Vehicle Based on ECMS in Intelligent Transportation Environment. *IFAC-Pap.* **2021**, *54*, 157–162. [CrossRef]
2. Wu, Z.; Xiang, Y.; Li, M.; Iqbal, M.Y.; Xu, G. Investigation of Accumulator Main Parameters of Hydraulic Excitation System. *J. Coast. Res.* **2019**, *93*, 613–622. [CrossRef]
3. Chen, L.; Geng, C.; Huang, J.; Wang, J. Modeling and Simulation of a New Transmission Structure for Heavy-Duty Hybrid Electric Vehicles. *Comput. Simul.* **2019**, *36*, 74–77+152.
4. Jeong, K.; Choi, S.B.; Choi, H. Sensor Fault Detection and Isolation Using a Support Vector Machine for Vehicle Suspension Systems. *IEEE Trans. Veh. Technol.* **2020**, *69*, 3852–3863. [CrossRef]
5. Nie, C.; Shao, Y.; Mechefske, C.K.; Cheng, M.; Wang, L. Power Distribution Method for a Parallel Hydraulic-Pneumatic Hybrid System using a Piecewise Function. *Energy* **2021**, *233*, 121033. [CrossRef]
6. Hemmati, S.; Doshi, N.; Hanover, D.; Morgan, C.; Shahbakhti, M. Integrated cabin heating and powertrain thermal energy management for a connected hybrid electric vehicle. *Appl. Energy* **2021**, *283*, 116353. [CrossRef]
7. Shen, P.; Zhao, Z.; Guo, Q.; Zhou, P. Development of Economic Velocity Planning Algorithm for Plug-in Hybrid Electric Vehicle. *IEEE Trans. Intell. Transp. Syst.* **2021**, *23*, 5501–5513. [CrossRef]
8. Liu, H.; Jiang, Y.; Li, S. Design and downhill speed control of an electric-hydrostatic hydraulic hybrid powertrain in battery-powered rail vehicles. *Energy* **2019**, *187*, 115957. [CrossRef]
9. Chen, K.; Mao, Z.; Zhang, J.; Jiang, Z. Diesel Engine Fault Diagnosis Based on Stack Autoencoder Optimized by Harmony Search. *J. Mech. Eng.* **2020**, *56*, 132–140.
10. He, Y.; Zhang, Y.; Zhang, H.; Wu, W.; Duan, J. Simulation Analysis and Diagnosis on AC/DC Converter Fault in SHEV. *Electr. Meas. Instrum.* **2019**, *56*, 9–15.
11. Zhang, Y.; Ji, J.; Meng, X.; Xu, T. Engine Bearing Fault Diagnosis Based on Exponential Wavelet Threshold and PSO-DP-LSSVM. *Mach. Tool Hydraul.* **2020**, *48*, 196–200.
12. Zhou, S.; Walker, P.D.; Xiao, B.; Zhang, N. Modelling and Vibration Analysis of a Parallel Hydraulic Hybrid Vehicle. *IEEE Trans. Veh. Technol.* **2020**, *69*, 10710–10723. [CrossRef]

13. Liu, G.; Wang, L. A Safety Distance Automatic Control Algorithm for Intelligent Driver Assistance System. In Proceedings of the 5th International Conference on Intelligent, Interactive Systems and Applications (IISA2020), Shanghai, China, 25–27 September 2020; pp. 645–652. [CrossRef]
14. Tian, J.; Li, D.; Ye, L. Study on Braking Characteristics of a Novel Eddy Current-Hydraulic Hybrid Retarder for Heavy-Duty Vehicles. *IEEE Trans. Energy Convers.* **2020**, *35*, 1658–1666. [CrossRef]
15. Helian, B.; Chen, Z.; Yao, B. Precision Motion Control of a Servo Motor-Pump Direct Drive Electro-hydraulic System with a Nonlinear Pump Flow Mapping. *IEEE Trans. Ind. Electron.* **2019**, *67*, 8638–8648. [CrossRef]
16. Kwak, J.; Kim, H.R. Performance analysis of magnetohydrodynamic pump for sodium-cooled fast reactor thermal hydraulic experiment. *Ann. Nucl. Energy* **2019**, *132*, 191–198. [CrossRef]
17. Shi, Q.; Zhang, H. Fault Diagnosis of an Autonomous Vehicle with an Improved SVM Algorithm Subject to Unbalanced Datasets. *IEEE Trans. Ind. Electron.* **2020**, *68*, 6248–6256. [CrossRef]
18. Hu, K.; Jiang, M.; Zhang, H.; Cao, S.; Guo, Z. Design of fault diagnosis algorithm for electric fan based on LSSVM and Kd-Tree. *Appl. Intell.* **2021**, *51*, 804–818. [CrossRef]
19. Han, Y.; Liu, B.; Wang, W.; Liu, F.; Zhang, J. Research on Fault Diagnosis of Diesel Electric Hybrid Based on Support Vector Machine. *Chin. Intern. Combust. Engine Eng.* **2022**, *43*, 101–108.
20. Li, G.; Görges, D. Energy management strategy for parallel hybrid electric vehicles based on approximate dynamic programming and velocity forecas. *J. Frankl. Inst.* **2019**, *356*, 9502–9523. [CrossRef]
21. Kuang, S. Simulated analysis of hybrid electric vehicle powertrain based on ADVISOR. In Proceedings of the RICAI 2020: The 2020 2nd International Conference on Robotics, Intelligent Control and Artificial Intelligence, New York, NY, USA, 17–19 October 2020; pp. 350–354.
22. Yang, L.M.; Tang, Z.M.; Liu, S.J. Research on optimisation method for project site selection based on improved genetic algorithm. *Int. J. Ind. Syst. Eng.* **2022**, *3*, 309–324. [CrossRef]
23. Meng, Z.; Zhang, H.; Yang, J.; Zhao, Q. Research on Matching of Power Transmission System of Electro-Hydraulic Hybrid Electric Vehicle. *IOP Conf. Ser. Earth Environ. Sci.* **2021**, *632*, 032007. [CrossRef]